Effect of Ni^{2+} and Cu^{2+} dopants on SnO_2 semiconductor nanoparticles synthesized by facile hydrothermal technique and their optical properties

K. ANANDAN
Department of Physics, AMET University, Chennai – 603 112, Tamilnadu, India

Pure and doped (Ni^{2+} and Cu^{2+}) SnO_2 nanoparticles was successfully synthesized by facile hydrothermal technique. The particles size, structure, morphology and composition of the samples were characterized by X-ray powder diffraction (XRD), Fourier transform infrared (FTIR) spectroscopy, scanning electron microscopy (SEM), transmission electron microscopy (TEM), high-resolution transmission electron microscopy (HR-TEM) and energy dispersive X-ray analysis (EDX) spectroscopy. The optical properties of the samples were analyzed by ultraviolet–visible (UV-vis) and photoluminescence (PL) spectroscopy. The optical band gap energies of pure, Cu and Ni doped SnO_2 nanoparticles were calculated to be 3.76, 3.83 and 3.87 eV, respectively. The PL emission spectrum shows that a strong luminescence peak located at 397 nm, which can be attributed to the near band-to-band edge transition recombination of electron-hole pairs. The smaller particle size of SnO_2 nanoparticles showed apparent quantum confinement effects. Finally, the mechanism for the formation of quantum size SnO_2 was also discussed.

(Received January 09, 2013; accepted June 09, 2016)

Keywords: Semiconductors, SnO_2, Dopants Effect, Structural studies, Morphological studies

1. Introduction

Tin oxide (SnO_2) has a tetragonal structure, with a wide band gap of E_g=3.6 eV, and behaves as an n- type semiconductor [1]. The optical properties of tin oxide are of great importance from the technological point of view and it has recently been a subject of great interest. Because of its good optical properties (transparent for visible light and reflective for IR) allied to good chemical and mechanical stability, it is commonly used in many applications such as oxidation catalysis, gas sensing, transparent conducting oxides and optoelectronic devices [2-5]. The optical properties of SnO_2 nanostructures can be enhanced by several ways like impurity doping, coating with surfactants and annealing. One of the most important methods to modify the characteristics of the materials is the introduction of dopants in the parent system. Many results have shown that several dopants can lead to an increase of surface area of SnO_2 by reducing the grain size and crystallanity. Tin oxide nanoparticles have been prepared by various techniques such as sol-gel method, chemical vapor deposition, pulsed laser deposition, plasma based evaporation, solvothermal, hydrothermal, co-precipitation and spray pyrolysis. Compared with other methods, the hydrothermal approach is a better alternative, with the advantages of mild synthetic conditions, simple manipulation and low pollution. Ethylenediamine is usually used as the structure direction agent for the synthesis of the 1D nanomaterial in the hydrothermal process, due to its strong chelating ability with metal ions, and numerous semiconductors with several morphologies were synthesized by using ethylenediamine as the solvent [6]. In this process, ethylenediamine was acted as a template molecule, which was incorporated into the inorganic framework first and then escaped from it to form nanocrystallites with the desired morphologies [6].

In this work, pure and doped (Cu and Ni) doped SnO_2 nanoparticles was prepared through the facile hydrothermal technique. A systematic study is presented for detailed characterization of the structure, morphology, composition and optical properties of the samples. Furthermore, the possible mechanisms for the formation of quantum sized Cu and Ni-doped SnO_2 nanoparticles were discussed.

2. Experimental procedure

2.1 Synthesis of pure and metal ion doped SnO_2 nanoparticles

All the chemical reagents used in the experiments were of an analytical grade and without further purification. Ni, Cu doped and Pure SnO_2 nanoparticles were synthesized; 1g of $SnCl_4.5H_2O$ was dissolved in 80ml of distilled water. While stirring vigorously, appropriate amount of transition metal ions ($Ni(CH_3COO)_2.4H_2O$/$Cu(CH_3COO)_2.H_2O$) was added and after few minutes 0.8 ml of ethylenediamine was slowly dropped into the above solution; slurry-like white precipitates were formed. After a few minutes of stirring, the solution was poured into a stainless steel Teflon-lined 100ml capacity of autoclave. Then, the autoclave was maintained at 200°C for 24 h, and then air-cooled to room temperature. The brownish colored precipitate was

repeatedly washed with distilled water and absolute ethanol several times, to remove the impurities and reduce the aggregation effect. The final product was dried in a vacuum at 60°C for 5h to obtain tin oxide nanoparticles. For comparison, pure SnO_2 nanoparticles were also synthesized with the same procedure without addition of transition metal ions.

2.2 Characterization of pure and metal ion doped SnO_2 nanoparticles

The crystalline size and structures of the samples were characterized by powder X-ray diffraction data were collected with a Seifert (JSO-DEBYFLEX 2002) powder diffractometer with copper target, and Cu Ka radiation (λ=0.1540 nm) was used for the phase identification, where the diffracted X-ray intensities were recorded as a function of 2θ. Fourier transformed infrared spectra, in the range of 4000–400 cm^{-1}, were recorded on the Nicolet 205 spectrometer. The surface morphologies of the products were studied using the Hitachi S-4500 scanning electron microscope. The particle size and morphology of the samples were further confirmed, and the corresponding Selected Area Electron Diffraction (SAED) patterns were examined by JEOL-3010 electron microscope operating at 120 kV (accompanied by energy dispersive X-ray analysis attachment for the compositional analysis). In the process of preparation of the TEM specimen, a small amount of the powders was dispersed in a few milliliters of ethanol in an ultrasonic bath, and ultrasonically treated for 30 minutes, and a drop from an eye dropper of the resulting suspension was placed onto a carbon-coated copper grid. The samples were placed in a vacuum oven to dry at ambient temperature before examining them. The sample was scanned in all the zones before the picture was taken. UV–visible absorption spectra were obtained from a Varian Cary 5E spectrophotometer. Photoluminescence spectra measurements were carried out on a Fluoromax-4 spectrofluorometer with a Xe lamp as the excitation light source

3. Results and discussion

Fig. 1 represents the powder X-ray diffraction patterns of Ni, Cu doped and pure SnO_2 nanoparticles respectively. Characteristic peaks with intensities corresponding to (110), (101), (211) and (301) planes were observed, which indicate that the sample is of high purity with tetragonal SnO_2 structure. It is clear that there are no extra peaks due to copper or nickel metal oxides implying that the transition metal ions get substituted at the Sn site without changing the tetragonal structure [7]. By using Scherrer's formula, the average crystallite size is calculated to be ~2.57, 5.12 and 6.58 nm for Ni^{2+}, Cu^{2+} doped and pure SnO_2, respectively. On doping, as the metal ions occupy the regular lattice site in SnO_2, the interference takes place between Ni and Cu-doped metal ions and those of SnO_2 lattice, due to the crystalline behaviour of the doped SnO_2 nanoparticles. Since, the ionic radius of Sn^{4+} (0.76Å) ion is larger than that of metal dopants Ni^{2+} (0.69Å) and Cu^{2+} (0.73Å) ions; hence the decrement in crystallite size was obtained. The FTIR is usually employed as an additional probe to evidence the presence of OH groups as well as other organic and inorganic species. Fig. 2 shows the FTIR spectra of Ni, Cu doped and pure SnO_2 nanoparticles. The intense broad bands located at ~3500, 1618 and 1098 cm^{-1} can be attributed to the O–H vibration in absorbed water on the sample surface. The broad bands between 450 and 790 cm^{-1} are attributed to the framework vibrations of the Sn–O bond in SnO_2 [8]. The peak appeared at ~700 cm^{-1} relates to the O–Sn–O bridge functional groups of SnO_2, which confirms the presence of SnO_2 as crystalline phase. This is consistent with the results of the XRD analysis. The SEM images reveal that the SnO_2 nanoparticles are small grains and the size of the particle is not homogeneous shown in Fig. 3(a-c). All the images showed the presence of aggregates composed of smaller individual particles in the coalesced form. The particle size ranges obtained from the SEM data were ~2-4nm (Ni), ~3-6 nm (Cu) and ~4–8nm (pure) respectively. It is thus clear that on incorporation of Ni^{2+} and Cu^{2+}, the particle size of SnO_2 reduces suggesting that the dopant influences the grain growth of SnO_2 nanoparticles.

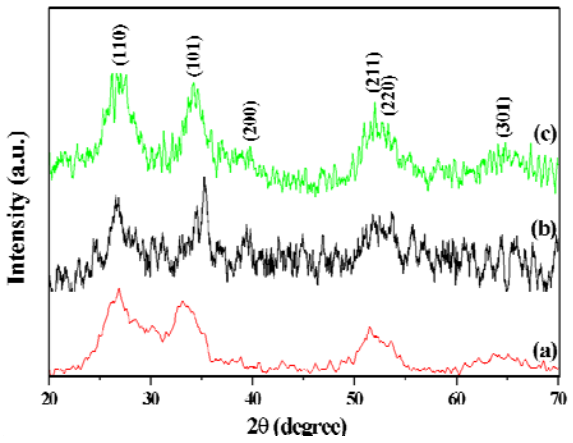

Fig.1. XRD pattern of (a) Ni, (b) Cu doped and (c) pure SnO_2 nanoparticles.

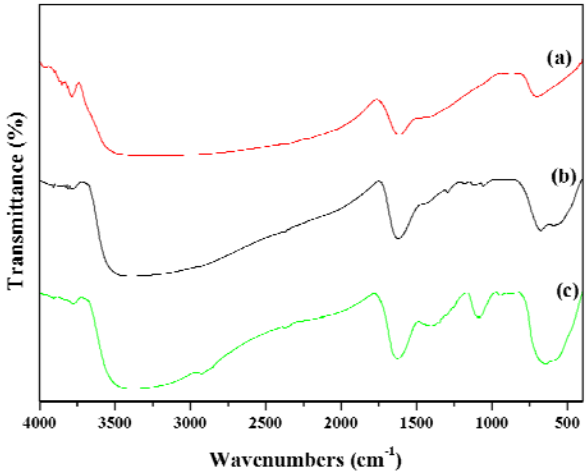

Fig.2. FTIR pattern of (a) Ni, (b) Cu doped and (c) pure SnO_2 nanoparticles.

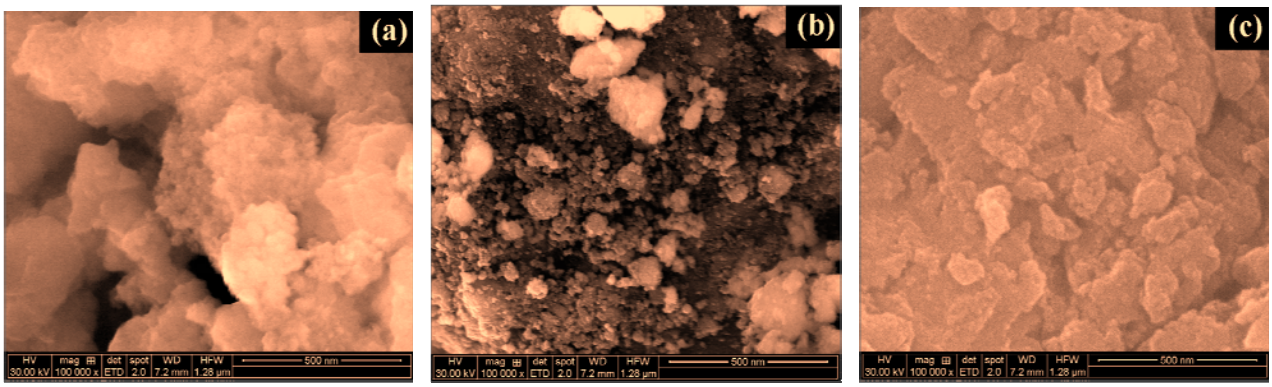

Fig.3. SEM images of (a) Ni, (b) Cu doped and (c) pure SnO_2 nanoparticles.

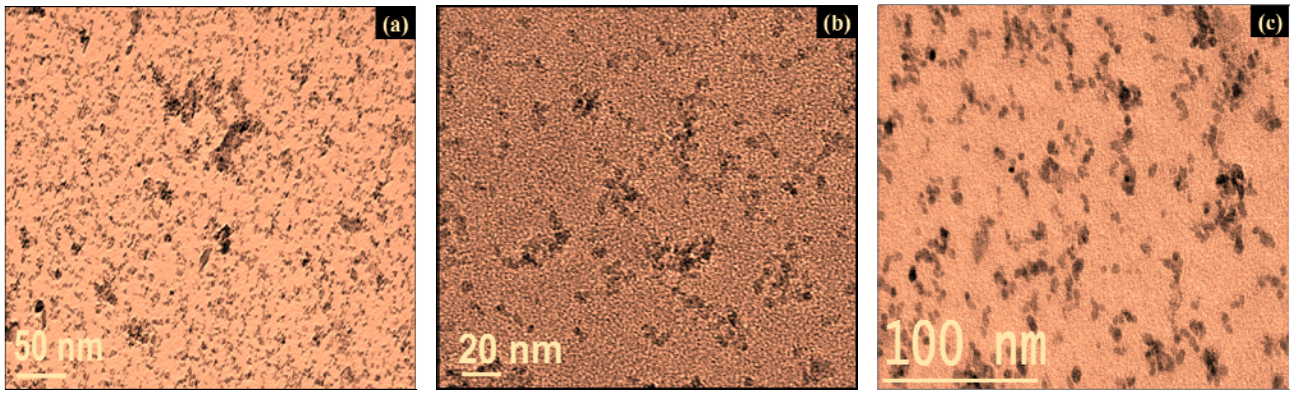

Fig.4. TEM images of (a) Ni, (b) Cu doped and (c) pure SnO_2 nanoparticles

The TEM analysis was carried out to further confirm the actual size and morphology of the samples. As demonstrated from the well dispersed nanoparticles shown in Fig. 4, the morphology of Ni, Cu doped and pure SnO_2 nanoparticles, which are spherical-like morphology. The individual particle sizes are found to be 2.5, 5 and 6.5 nm for Ni, Cu doped and pure SnO_2 nanoparticles, respectively, which are good agreement with XRD results. The high-resolution transmission electron microscopy (HR-TEM), selected area electron diffraction (SAED) pattern and energy dispersion X-ray (EDX) spectrum of Ni doped individual SnO_2 nanoparticle shown in Fig. 5a-c. HR–TEM lattice fringes, indicating the established crystallinity of SnO_2 nanoparticles. The distance between lattice fringes was found to be 0.33 nm, which was in good agreement with the lattice spacing of (110) plane in the SnO_2. SAED pattern represents a collection of halo-rings; confirm the poly-crystalline nature, tetragonal structure of the SnO_2 nanoparticles, which agrees with the powder XRD results. The EDX spectrum is used to confirm the composition of the samples. The image showed the presence of Sn, O and Ni as the only elementary species in the sample, which indicates that high purity of the product and Ni ion successfully incorporated with SnO_2 nanoparticles.

The optical band gap energy (E_g) of the samples was estimated from the Tauc curves by plotting $(\alpha h\nu)^2$ versus the photon energy ($h\nu$). In order to calculate the direct band gap, the Tauc relation was used:

$$\alpha h\nu = A(h\nu - E_g)^n$$

where α is the absorption coefficient, A is a constant relative to the material, and n=1/2 for the direct band gap semiconductor. The energy gap is obtained by fitting the linear part of the curve and finding the intersection of the straight line with the $h\nu$ axis as shown in Fig. 6. The determined band gap (E_g) values of Ni, Cu doped and pure SnO_2 nanoparticles were 3.87, 3.83 and 3.76 eV, respectively, which are higher than the reported value of bulk SnO_2, i.e. 3.6 eV [1]. It is well known that semiconductors of nanoscale size show a blue shift in their spectra due to the quantum confinement effects. It is noticed that the phenomenon of the blue shift, with the increase of the band gap value, is an evidence of the quantum confinement effect.

It is clear that the particle size decreases when the band gap increases; the increase in the band gap suggests that the size of the nanoparticles influences the optoelectronic properties of the materials, and can be tuned by the doping.

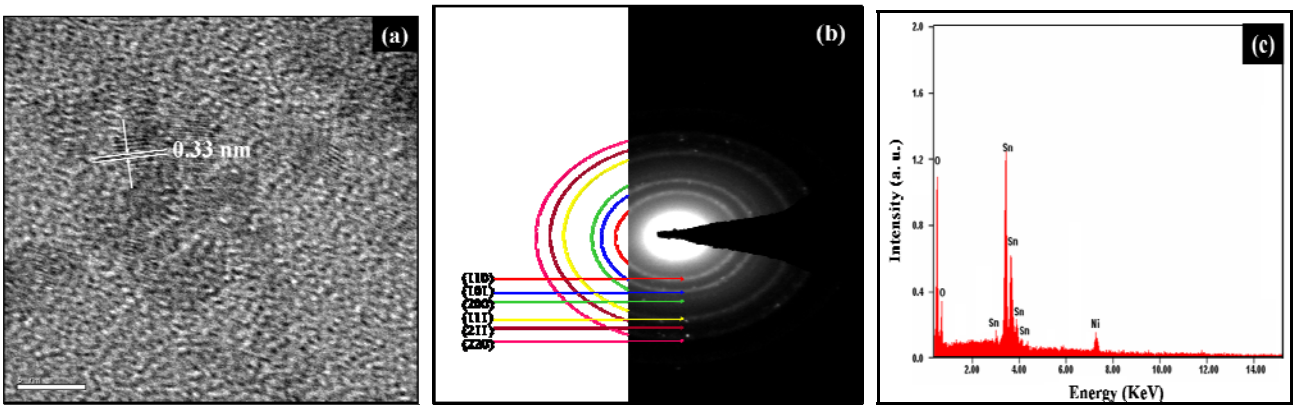

Fig. 5. HR-TEM, SAED and EDX spectrum of Ni doped SnO_2 nanoparticle.

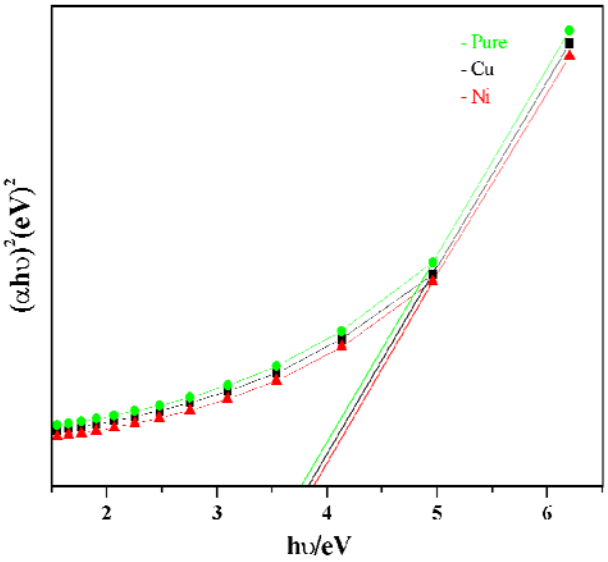

Fig. 6. $(\alpha h\nu)^2$ vs. $h\nu$ curve of the SnO_2 nanoparticles

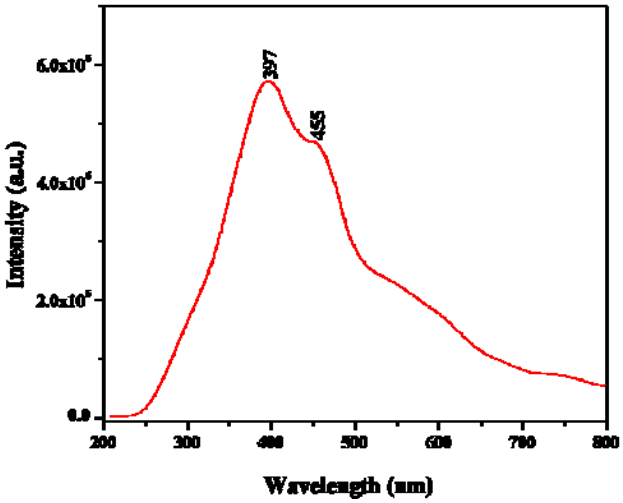

Fig. 7. PL spectrum of Ni doped SnO_2 nanoparticles.

Fig. 7 shows the PL emission spectrum of Ni doped SnO_2 nanoparticles an excitation wavelength of 275 nm. One strong and broad peak, centered at 397 nm, can be attributed to near band-to-band transition. Another one shoulder peak, centered at 455 nm, can be assigned to oxygen-related defects [9] introduced during hydrothermal growth. The visible emission can be related to defect levels within the band gap of SnO_2 associated with different types of oxygen vacancies or Sn interstitials that have formed during the synthesis process. The interactions between oxygen vacancies and interfacial tin vacancies lead to the formation of a significant number of trapped states, which form a series of metastable energy levels within the band gap and result in emission in the visible region. There is a profound increment in the intensity of the peak due to the Ni ion doping effect [10, 11]. This result is well matched with the absorbance spectra and is consistent with our observations.

Generally, oxygen vacancies are known to be the most common defects in semiconductor nanocrystals and usually act as radiative center of luminescence in visible region. In SnO_2, oxygen vacancies are present in three different charge states: V^0_o, V^+_o and V^{++}_o, in which V^0_o is very shallow donor. The origin of visible emission can be assigned to the recombination of electrons in the shallow levels with the photo excited holes in valence band. Ni ion doped samples, it is easy for Ni^{2+} ion to substitute for Sn^{4+} ion because the ionic radius of Ni^{2+} and Sn^{4+} are almost equal, In addition, -2 charge of the substituted Sn site has to be compensated from somewhere in the lattice in the form of oxygen vacancy. The vacancy thus created give rise to defect levels in the crystal and hence enhances the visible emission in the photoluminescence spectrum.

It is well known that ethylenediamine is both a strong coordination that can coordinate with Sn^{4+} and a strong alkali reagent. Fig. 1(a–c) shows the XRD patterns of samples, the particles diameter drastically decreased from pure to Ni doped SnO_2, which were confirmed by the TEM analyses. The Fig.6 clearly show the decreasing particles size upon the increasing of the band gap energy, it confirms the quantum effect. From the above results, the

possible mechanism for formation of quantum-size SnO_2 nanoparticles during the hydrothermal process was as follows: as the ethylenediamine was added into the precursor solutions, the complex of $Sn_n(ethylenediamine)_m^{4+}$ were formed immediately and a white slurry was observed. Mean while, –OH groups were released. During the hydrothermal process, the complex of $Sn_n(ethylenediamine)_{m-x}(OH)_x^{(4-x)+}$ were dissociated and SnO_2 nanoparticles formed gradually. It was thought that the formation of $Sn_n(ethylenediamine)_m^{4+}$ complex decreased the reactivity between the Sn ion and the –OH group, resulting in the formation of quantum sized SnO_2 nanoparticles [12].

4. Conclusions

The pure and doped (Ni^{2+} and Cu^{2+}) SnO_2 nanoparticles have been successfully synthesized by facile hydrothermal technique. The structural characterization of the samples was studied, by using the XRD and FTIR, which revealed a tetragonal phase for the host material. A spherical morphology of the prepared pure and doped-SnO_2 nanoparticles was confirmed by the SEM and TEM studies, with sizes in the range of 2.5- 6.5 nm. It was found that the dopants played an important role in the particle size effect of nanocrystalline SnO_2. The PL emission spectrum shows that a strong and shoulder luminescence peaks at 397 and 455 nm, which may be attributed to near band-to-band transition and oxygen-related defects. Hence, with respect to the structural and optical properties; they could be useful for nanoscaled technological applications such as optoelectronic devices.

References

[1] Z.R. Dai, Z.W. Pan, Z.L. Wang, Adv. Funct. Mater. **13**, 9 (2003).
[2] S. D. Monredon, A. Cellot, F. Ribot, C. Sanchez, L. D. Armelao, L. Guanean, L. Delattre, J. Mater. Chem. **12**, 2396 (2002).
[3] N. Sergent, P. Gelin, L. P. Camby, H. Praliaud, G. Thomas, Sensors and Actuators B: Chemical, **84**, 176 (2002).
[4] T. T. Emons, J. Li, L. F. Nazar, J. Am. Chem. Soc. 124, 8516 (2002).
[5] F. Gu, S. F. Wang, M. K. Lu, Y. X. Qi, G. J. Zhou, D. Xu, D. R. Yuan, Optical Materials, **25**, 59 (2004).
[6] Z.X. Deng, C. Wang, X.M. Sun, Y.D. Li, Inorg. Chem. **41**, 869 (2002).
[7] B. Esfandyarpour, S. Mohajerzadeh, S. Famini, A. Khodadadi, E. Asl Soleimani, Sensors and Actuators B, **100**, 190 (2004).
[8] J. Zhang, L. Gao, J. Solid State Chem. **177**, 1425 (2004).
[9] B. Chen, J.M. Russell, W.S. Shi, L. Zhang, E.T. Samulski, Large-Scale, J. Am. Chem. Soc. **126**, 5972 (2004).
[10] M.H. Huang, Y. Wu, H. Feick, N. Tran, E. Weber, P. Yang, Adv. Mater. **13**, 113 (2001).
[11] Q. Tang, W. Zhou, J. Shen, W. Zhang, L. Kong, Y. Qian, Chem. Commun. **2**, 712 (2004).
[12] Y. Liu, F. Yang, X. Yang, Colloid. Surf. A **312**, 219 (2008).

*Corresponding author: anand.nanoscience@yahoo.com;
anandphy1@yahoo.com